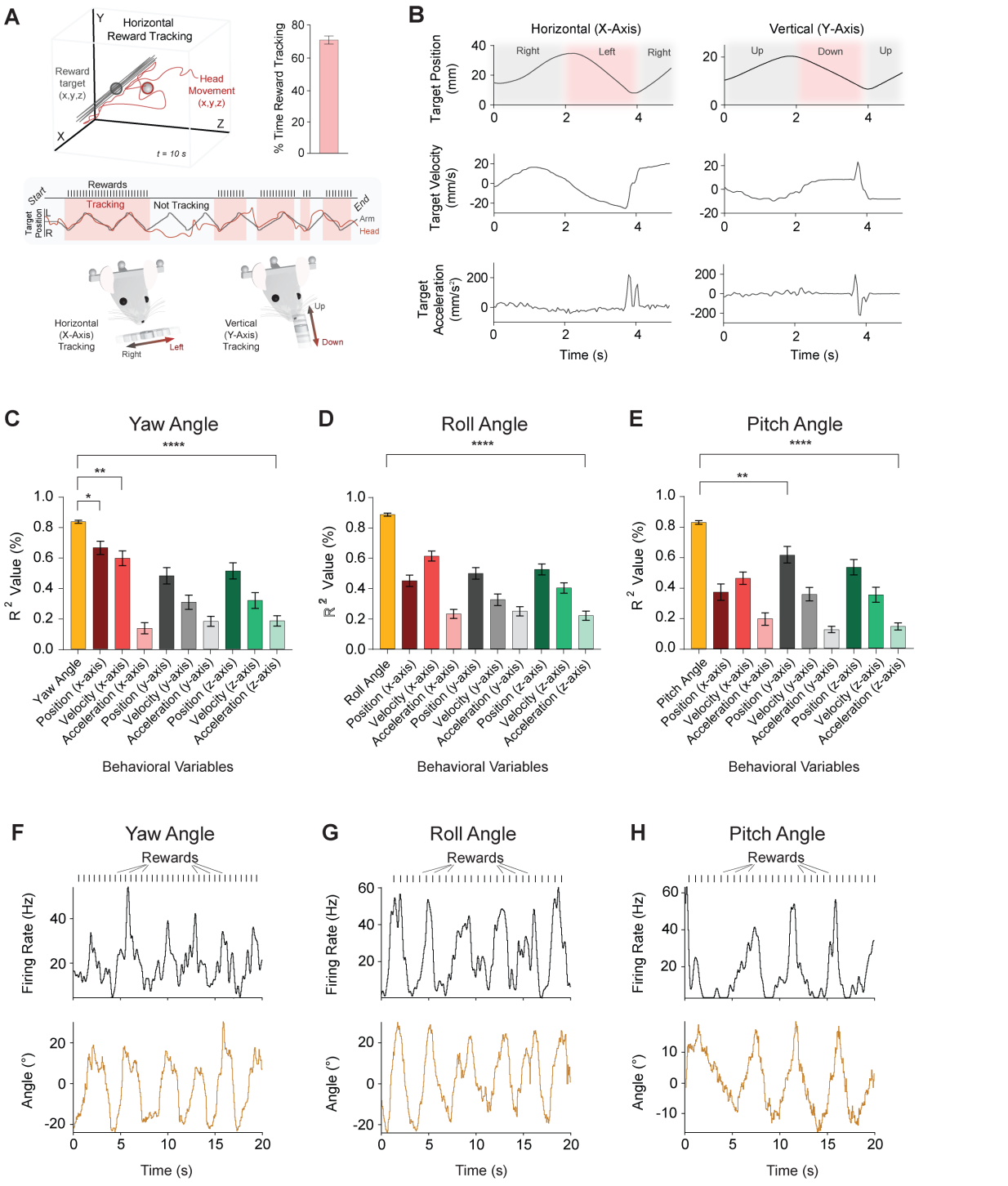

Figure S1. Behavioral task description and analyses for all other behavioral variables from pitch, roll and yaw neurons. Related to Figure 2.

(A) Illustration of the reward tracking task with 3D motion capture. When the spout begins to move in either the vertical or horizontal direction, mice receive a reward if they are within a narrow window of Cartesian space. When they cease tracking, no more rewards are delivered. Mice spent on average 71 % of time tracking the spout (0.71 ± 0.03; Mean and SEM).
(B) The target spout moved with a variable velocity throughout the session. *Top*) Graph of the spout position over time for both horizontal (*left)* and vertical (*right*) tracking. *Middle*) Graph of the spout velocity over time for both horizontal (*left)* and vertical (*right*) tracking. *Bottom*) Graph of the spout acceleration over time for both horizontal (*left)* and vertical (*right*) tracking.
(C-E) Correlation between other relevant behavioral variables and pitch, roll and yaw neurons showing a significant difference between all other behavioral variables.
(C) Neurons classified as Yaw angle neurons had a significantly higher correlational value than all other behavioral variables (one-way ANOVA, $p < 0.05$, $n = 26$).
(D) Roll Angle neurons had a significantly higher correlational value compared to other behavioral variables (one-way ANOVA, $p < 0.05$, $n = 62$).
(E) Pitch angle neurons had a significantly higher correlational value than all other behavioral variables (one-way ANOVA, $p < 0.05$, $n = 36$). (* indicates p value adjusted for multiple comparisons using Dunnett's multiple comparison's test. * $p < 0.05$; ** $p < 0.01$; **** $p < 0.0001$).
(F-H) Raw neural traces with their respective angle from a random 20 second window with corresponding reward times. Individual neurons did not show a clear relationship with reward.
(F) A representative yaw angle neuron.
(G) A representative roll angle neuron.
(H) A representative pitch angle neuron.

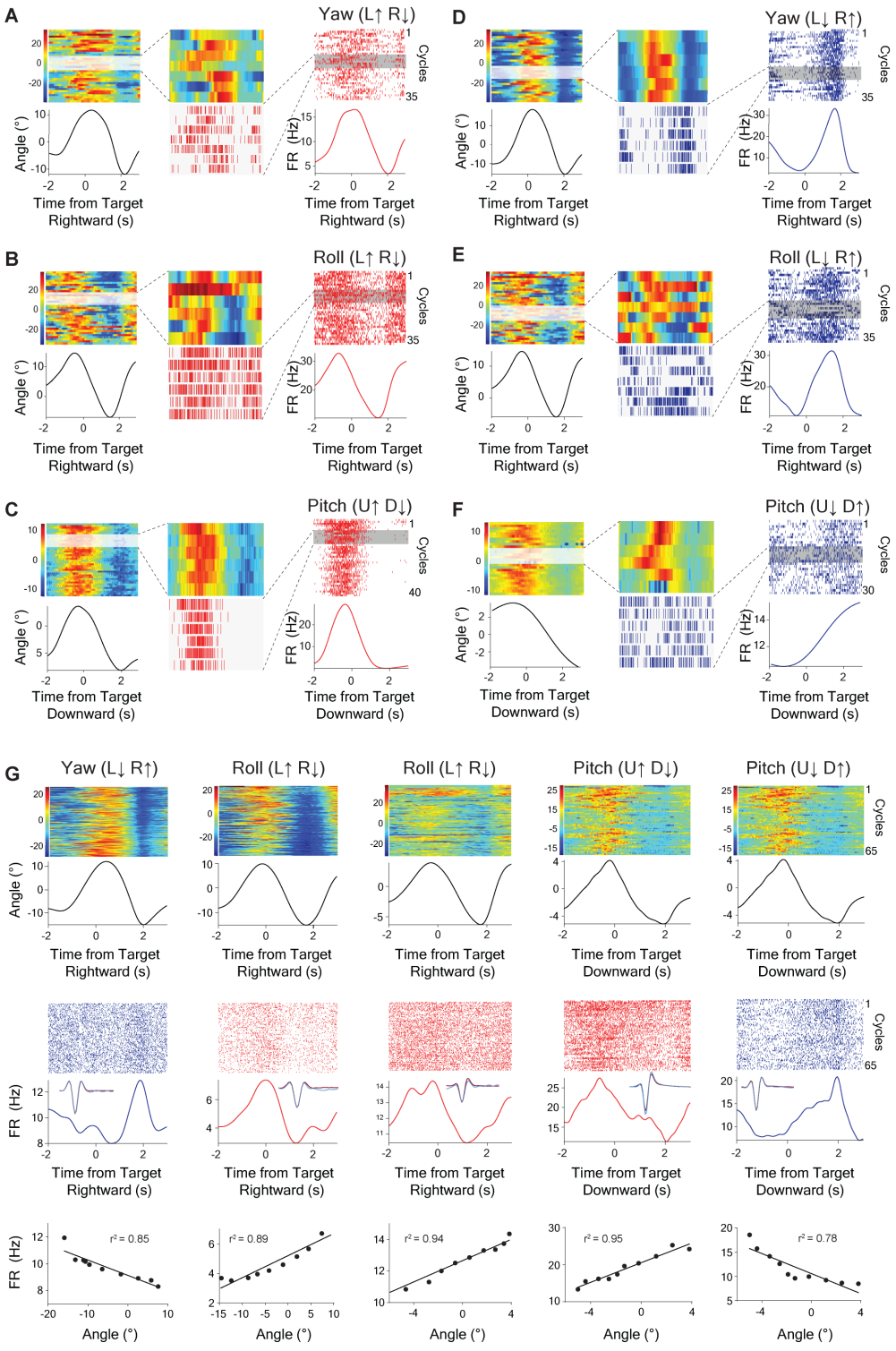

Figure S2. Detailed results from representative neurons in Figure 1 and optogenetically tagged neurons. Related to Figure 2.

(A-F) Single cycle examples demonstrating the robust correlation between neural activity and head angle**.** Head angle is on the left and VTA GABAergic neural activity is on the right. Select cycles are shown in the middle.
(A) Single-cycle perievent rasters and corresponding behavioral traces for representative Yaw (L↑ R↓) neuron (7 cycles; *PC*, $r^2 = 0.89$, $p < 0.0001$).
(B) Single-cycle perievent rasters and corresponding behavioral traces for representative Roll (L↑ R↓) neuron (6 cycles; *PC*, $r^2 = 0.99$, $p < 0.0001$).
(C) Single-cycle perievent rasters and corresponding behavioral traces for representative Pitch (U↑ D↓) neuron (6 cycles; *PC*, $r^2 = 0.93$, $p < 0.0001$).
(D) Single-cycle perievent rasters and corresponding behavioral traces for representative Yaw (L↓ R↑) neuron (6 cycles; *PC*, $r^2 = 0.80$, $p < 0.01$).
(E) Single-cycle perievent rasters and corresponding behavioral traces for representative Roll (L↓ R↑) neuron (7 cycles; *PC*, $r^2 = 0.98$, $p < 0.0001$).
(F) Single-cycle perievent rasters and corresponding behavioral traces for representative Pitch (U↓ D↑) neuron (7 cycles; *PC*, $r^2 = 0.91$, $p < 0.0001$).
(G) 5 out of the 18 optically tagged neurons fell into one of the six classes of neurons: 1 Yaw (L↓ R↑) neuron, 2 Roll (L↑ R↓) neurons, 1 Pitch (U↑ D↓) neuron, and 1 Pitch (U↓ D↑) neuron.

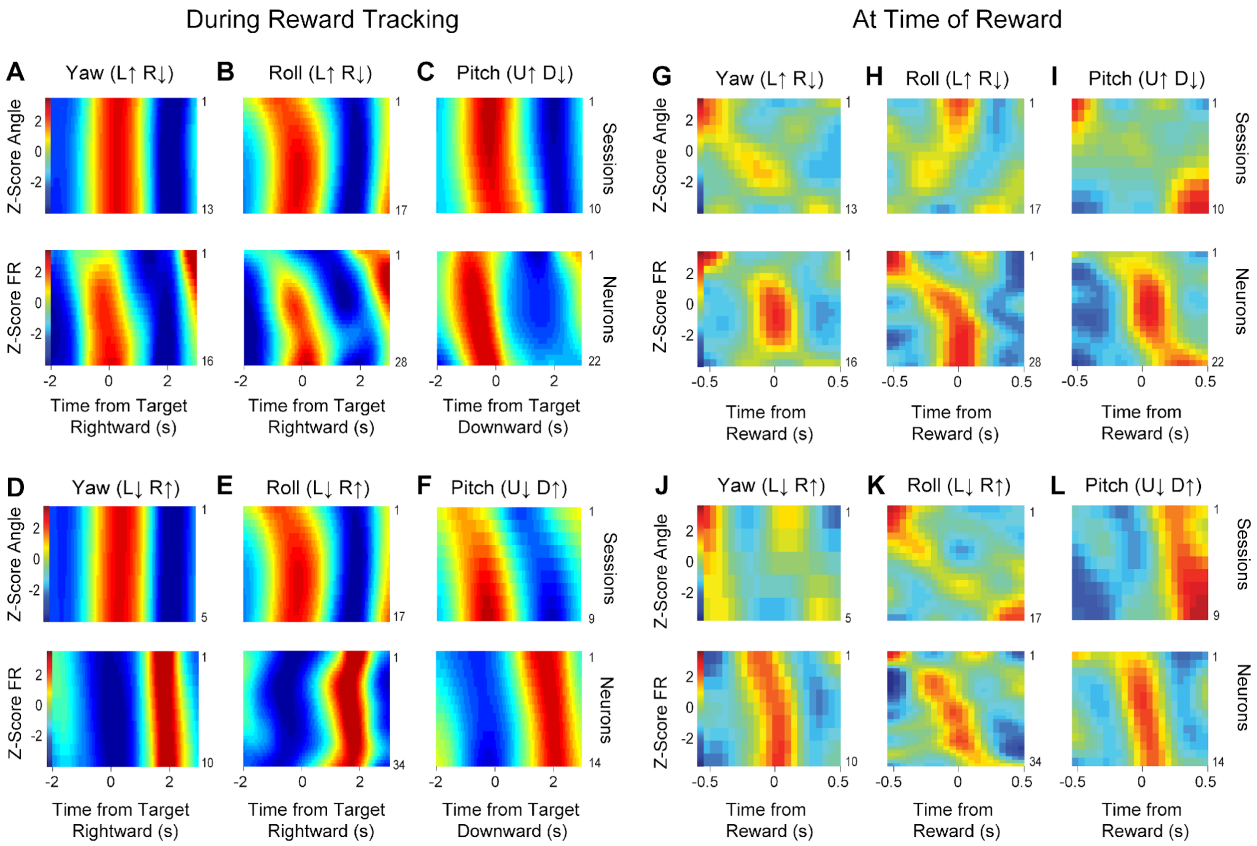

Figure S3. Population heat maps of electrophysiological data for yaw, roll and pitch during reward tracking and at the time of reward consumption. Related to Figure 2.

(A) Yaw (L↑ R↓) angle population heat maps during tracking behavior. *Top*) Normalized yaw angle across 13 behavioral sessions. *Bottom*) Normalized firing rate of Yaw (L↑ R↓) neurons (*n* = 16).

(B) Roll (L↑ R↓) angle population heat maps during tracking behavior. *Top*) Normalized roll angle across 17 behavioral sessions. *Bottom*) Normalized firing rate of Roll (L↑ R↓) neurons (*n* = 28).

(C) Pitch (U↑ D↓) angle population heat maps during tracking behavior. *Top*) Normalized pitch angle across 10 behavioral sessions. *Bottom*) Normalized firing rate of Pitch (U↑ D↓) neurons (*n* = 22).

(D) Yaw (L↓ R↑) angle population heat maps during tracking behavior. *Top*) Normalized yaw angle across 5 behavioral sessions. *Bottom*) Normalized firing rate of Yaw (L↓ R↑) neurons (*n* = 10).

(E) Roll (L↓ R↑) angle population heat maps during tracking behavior. *Top*) Normalized roll angle across 17 behavioral sessions *Bottom*) Normalized firing rate of Roll (L↓ R↑) neurons (*n* = 34).

(F) Pitch (U↓ D↑) angle population heat maps during tracking behavior. *Top*) Normalized pitch angle across 9 behavioral sessions *Bottom*) Normalized firing rate of Pitch (U↓ D↑) neurons (*n* = 14).

(G) Yaw (L↑ R↓) angle population heat maps at time of reward. *Top*) Normalized yaw angle across 13 behavioral sessions. *Bottom*) Normalized firing rate of Yaw (L↑ R↓) neurons (n = 16). **(H)** Roll (L↑ R↓) angle population heat maps at time of reward. *Top*) Normalized roll angle across 17 behavioral sessions. *Bottom*) Normalized firing rate of Roll (L↑ R↓) neurons (n = 28). **(I)** Pitch (U↑ D↓) angle population heat maps at time of reward. *Top*) Normalized pitch angle across 10 behavioral sessions. *Bottom*) Normalized firing rate of Pitch (U↑ D↓) neurons (n = 22). **(J)** Yaw (L↓ R↑) angle population heat maps at time of reward. *Top*) Normalized yaw angle across 5 behavioral sessions. *Bottom*) Normalized firing rate of Yaw (L↓ R↑) neurons (n = 10). **(K)** Roll (L↓ R↑) angle population heat maps at time of reward. *Top*) Normalized roll angle across 17 behavioral sessions *Bottom*) Normalized firing rate of Roll (L↓ R↑) neurons (n = 34). **(L)** Pitch (U↓ D↑) angle population heat maps. *Top*) Normalized pitch angle across 9 behavioral sessions *Bottom*) Normalized firing rate of Pitch (U↓ D↑) neurons (n = 14).

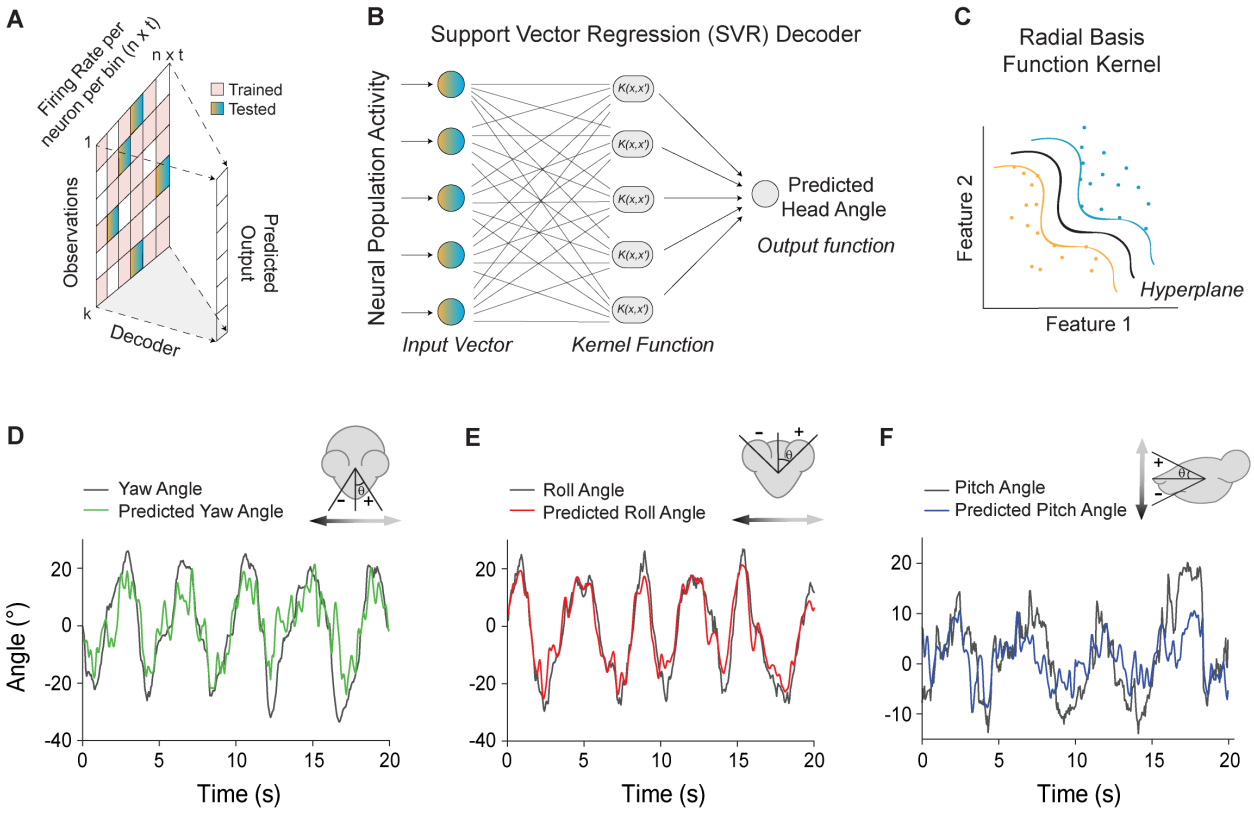

Figure S4. Neural activity accurately predicts head angle using a Support Vector Regression (SVR) decoder. Related to Figure 4.

(A) Schematic of a non-recurrent neural decoder used to predict head-angle. It takes the firing rate of all neurons, *n*, across all time bins (50 ms), *t*. The first 60 % of the data was used to train the model, and a contiguous 15% of held-out data was then used to test the model.
(B) A Support Vector Regression (SVM) fits a kernel function to an input vector in order to predict the output vector, in this case the continuous head-angle measurements.
(C) A non-linear radial basis function kernel was used as the kernel function in the SVR decoder, which analyses patterns within the data set and separates them into subspaces by finding a hyperplane in the high-dimensional feature space.
(D-F) Schematic illustration of the decoded head angle (*top*); Traces of head angle behavior during tracking, and the predicted head angle from the decoded neural activity (*bottom)*.
(D) Representative model test on predicted yaw angle versus actual yaw angle from GABA population.
(E) Representative model test on predicted roll angle versus actual roll angle from GABA population.
(F) Representative model test on predicted pitch angle versus actual pitch angle from GABA population.

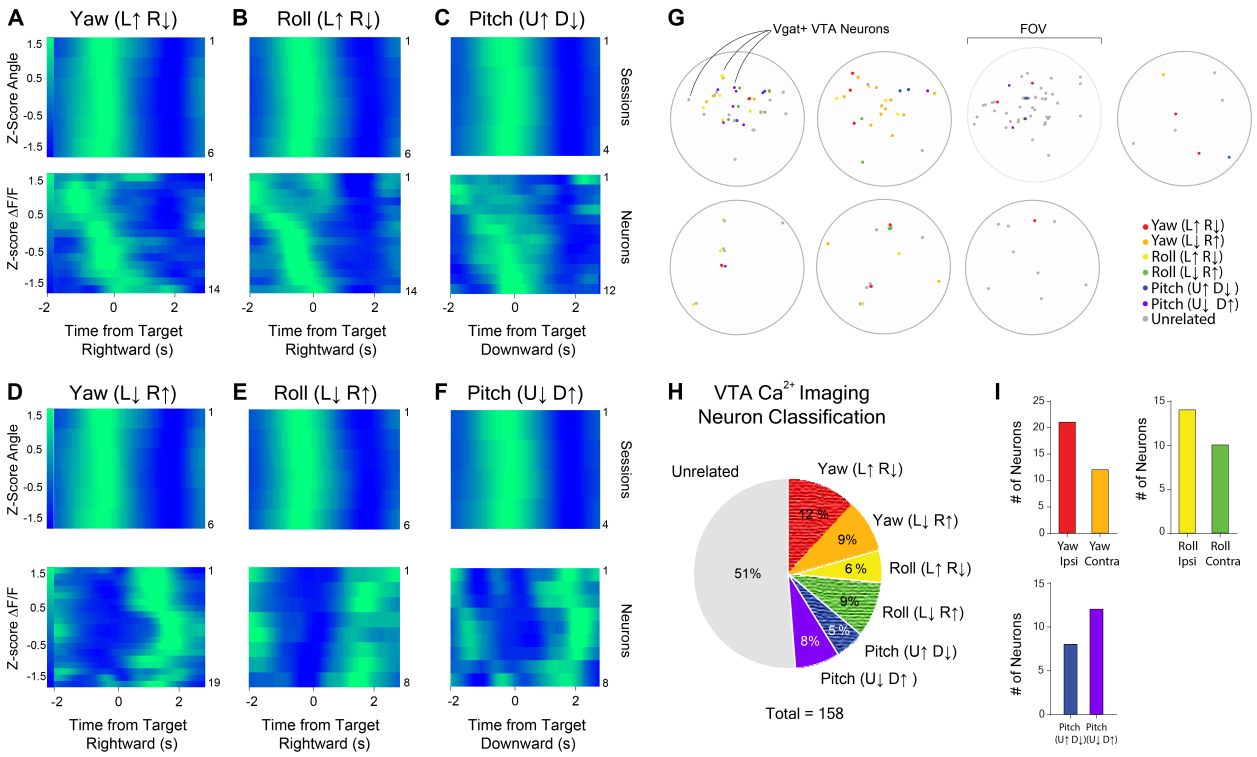

Figure S5. Population heat maps and summary of calcium imaging data for pitch, roll, and yaw. Related to Figure 5.

(A) Yaw (L↑ R↓) angle population heat maps. *Top*) Normalized yaw angle across 6 behavioral sessions. *Bottom*) Normalized ΔF/F of Yaw (L↑ R↓) neurons (n = 14).

(B) Roll (L↑ R↓) angle population heat maps. *Top*) Normalized roll angle across 16 behavioral sessions. *Bottom*) Normalized ΔF/F of Roll (L↑ R↓) neurons (n = 14).

(C) Pitch (U↑ D↓) angle population heat maps. *Top*) Normalized pitch angle across 4 behavioral sessions. *Bottom*) Normalized ΔF/F of Pitch (U↑ D↓) neurons (n = 12).

(D) Yaw (L↓ R↑) angle population heat maps. *Top*) Normalized yaw angle across 6 behavioral sessions. *Bottom*) Normalized ΔF/F of Yaw (L↓ R↑) neurons (n = 19).

(E) Roll (L↓ R↑) angle population heat maps. *Top*) Normalized roll angle across 6 behavioral sessions. *Bottom*) Normalized ΔF/F of Roll (L↓ R↑) neurons (n = 8).

(F) Pitch (U↓ D↑) angle population heat maps. *Top*) Normalized pitch angle across 4 behavioral sessions. *Bottom*) Normalized ΔF/F of Pitch (U↓ D↑) neurons (n = 8)

(G) Topographical distribution of angle neurons within each animal from calcium imaging data (n = 7).

(H) Breakdown of angle neuron percentages of calcium imaging neurons.

(I) Quantification of the number of Yaw angle neurons that increase their firing rate in the ipsiversive direction (n = 21) or contraversive direction (n = 12) in relation to the recording hemisphere (*top left*); the number of Roll angle neurons that increase their firing rate in the ipsiversive direction (n = 14) or contraversive direction (n = 10) in relation to the recording hemisphere (*top right*), and the number of Pitch angle neurons (*bottom left*) that increase their firing rate in the upward direction (n = 8) or downward direction (n = 12).

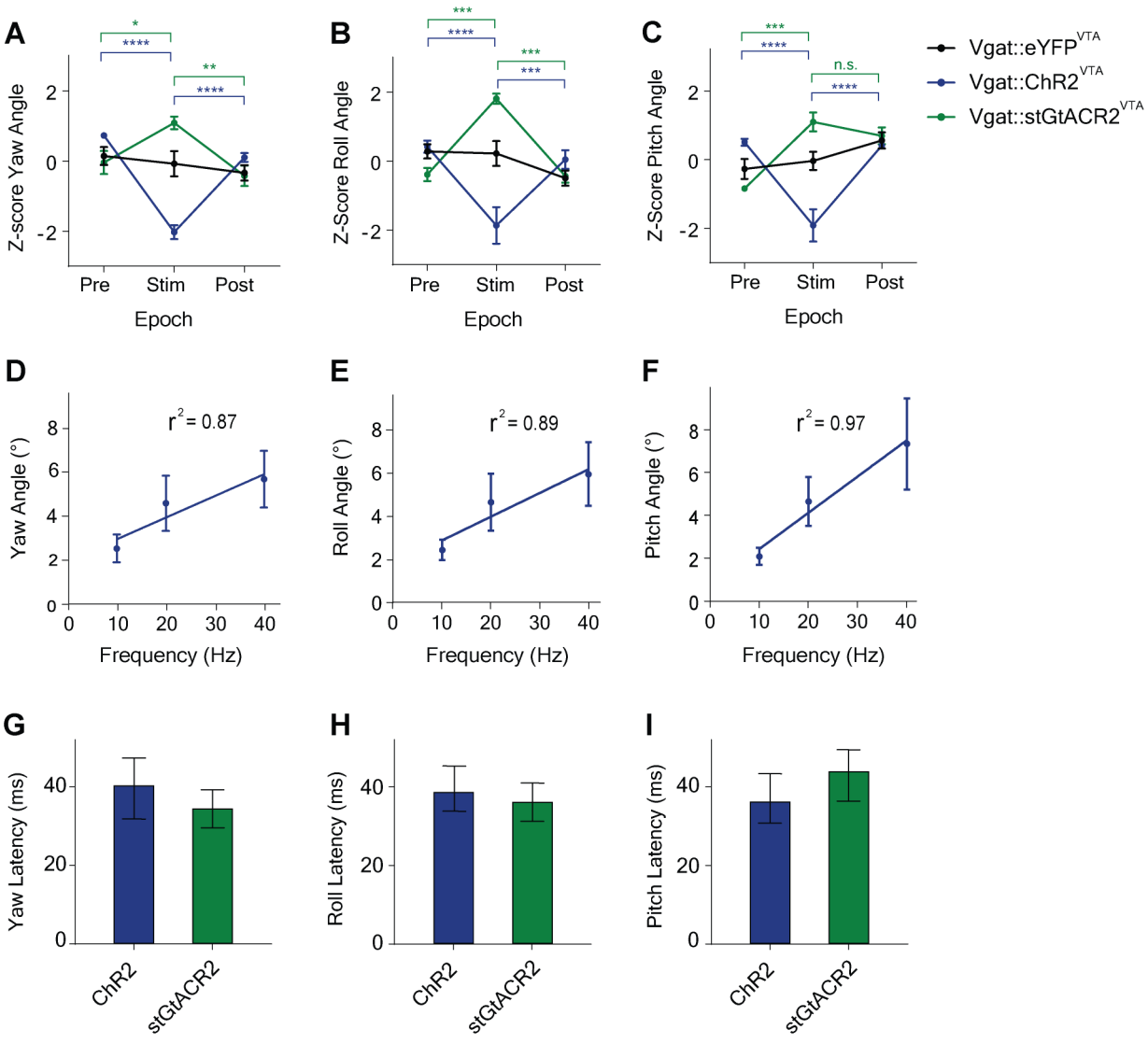

Figure S6. Summary of optogenetic experiments. Related to Figure 6.
(A) Deviations of yaw angle over time during 500 ms of optogenetic excitation, inhibition and control. Yaw angle was significantly different during optogenetic excitation and inhibition than during pre and post period compared to control group (two-way RM ANOVA; Yaw Angle, Main effect of Group, $F_{(2,16)} = 12.16$, $p = 0.006$).
(B) Roll angle before and after optogenetic stimulation (two-way RM ANOVA, Roll Angle, Main effect of Group, $F_{(2,16)} = 18.75$, $p < 0.0001$).
(C) Pitch angle before and after optogenetic stimulation (two-way RM ANOVA, Pitch Angle, Main effect of Group, $F_{(2,15)} = 12.20$, $p = 0.007$).
(D-F) There is a linear relationship between frequency of stimulation and head angle change.
(D) Yaw angle changes due to 10 Hz, 20 Hz and 40 Hz stimulation ($r^2 = 0.87$, $n = 5$).
(E) Roll angle changes due to 10 Hz, 20 Hz and 40 Hz stimulation ($r^2 = 0.89$, $n = 5$).
(F) Pitch angle changes due to 10 Hz, 20 Hz and 40 Hz stimulation ($r^2 = 0.97$, $n = 5$).
(G) Latency between optogenetic stimulation and deviation of yaw angle (37 ± 5 ms).
(H) Latency between optogenetic stimulation and deviation of roll angle (37 ± 4 ms).

(I) Latency between optogenetic stimulation and deviation of pitch angle (39 ms ± 6 ms). (* values reflect adjusted *p* values from Tukey's *post-hoc* pairwise comparisons. * $p < 0.05$; ** $p = 0.004$; *** $p < 0.001$; **** $p < 0.0001$).

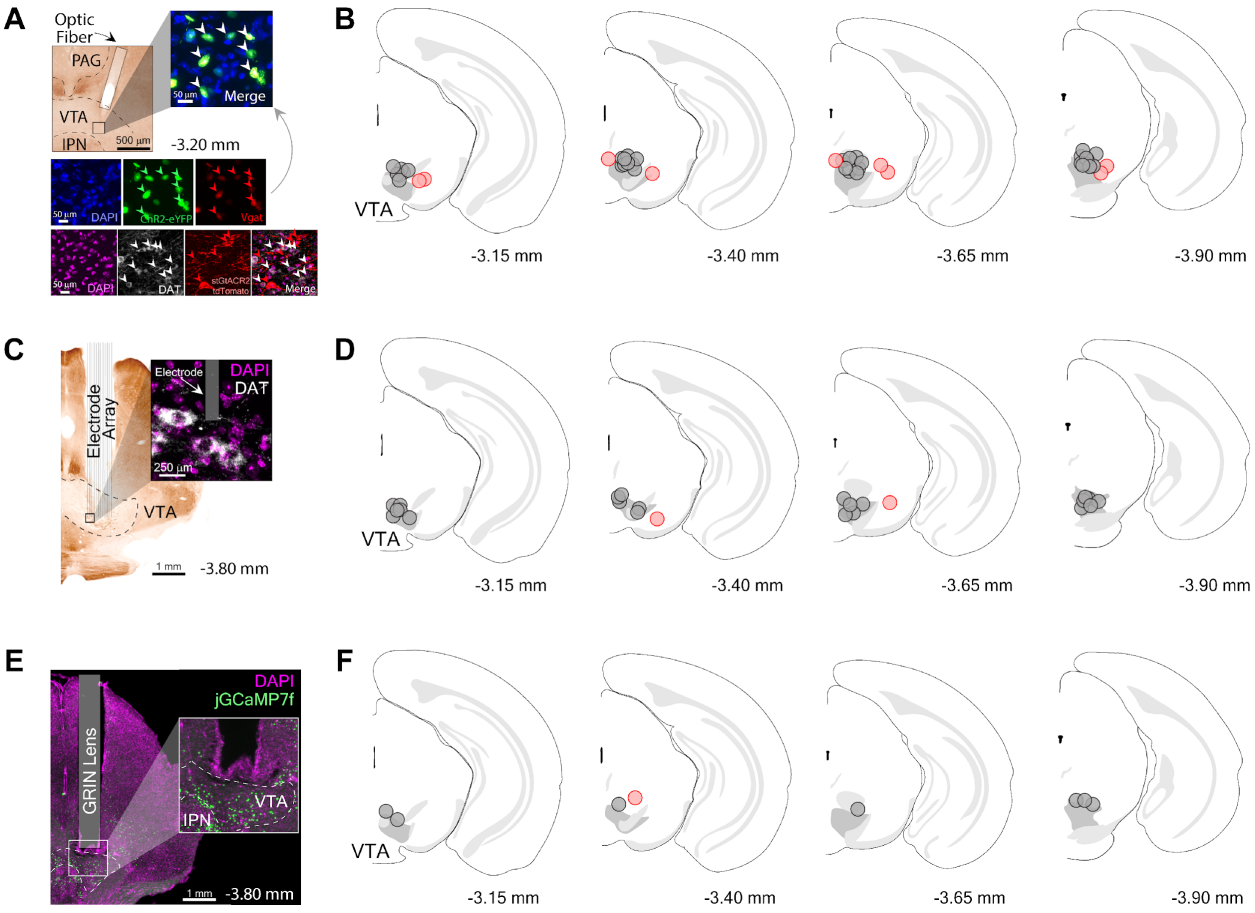

Figure S7. Histological verification of VTA placement. Related to Figures 1-2 and 5-6.
(A) Representative example of a coronal section through the midbrain showing optic fiber placement above the VTA. Inset shows eYFP infected Vgat+ neurons in the VTA.
(B) Optic fiber placements for VTA optogenetic experiments (n = 19).
(C) Representative example of coronal section through the midbrain showing electrode array placement into the VTA. Inset shows electrode tip co-localization with dopaminergic (DAT) neurons in the VTA.
(D) Electrode array placement into the VTA (n = 20).
(E) Representative example of coronal section showing GRIN lens placement above the VTA
(F) GRIN lens placement above the VTA for calcium imaging experiments (n = 7). Black circles indicate data points included in study. Red circles indicate excluded data points. Coordinates with respect to bregma are shown beneath coronal schematics.